Synthesis, characterization and structural refinement of a new phase $(1-x)BiO_{1.5}-(x/4)Nb_2Te_2O_9$ (x=0.1, 0.2), type δ-Bi_2O_3

L.LOUBBIDI[1]*, A.CHAGRAOUI[1], B.ORAYECH[2], A.MOUSSAOUI[1], A.TAIRI[1], O.AIT SIDI AHMED[1], J.M. IGARTUA[2], A.MENICHI[1]

(1) Laboratory of Physical Chemistry of Applied Materials (LPCMA), Faculty of Science Ben M'sik, University Hassan II-Casablanca (Morocco).
(2) Departamento de Fisica de la Materia Condensada, Universidad delPais, E-48080, Bilbao, Spain.

E-mail: leila.loubbidi@gmail.com

ABSTRACT

Original nano-stoechiometric oxides with formula $(1-x)BiO_{1.5}-(x/4)Nb_2Te_2O_9$ (x=0.1, 0.2, 0.3, 0.6 and 0.9) have been synthesized by solid state reaction at 850°C and characterized by powder X ray diffraction. The phases for (x=0.1, 0.2) belong to a cubic fluorite structure type δ-Bi_2O_3.

The pattern refinement of the composition (x=0.2): $Bi_{0.8}Nb_{0.1}Te_{0.1}O_{1.65}$ was carried out by means of the Rietveld using the FULLPROF program. It crystallizes in the cubic unit cell, space group Fm-3m and a lattice parameter a = 5.499Å. The reliability factors are R_F = 2.09% and R_B = 2.99%. The composition ranges and the evolution of the lattice parameter as a function of the substituting elements have been determined. The morphological proprieties of the new phases (x=0.1): $Bi_{0.9}Nb_{0.05}Te_{0.05}O_{1.575}$ and (x=0.2): $Bi_{0.8}Nb_{0.1}Te_{0.1}O_{1.65}$ have been investigated by means of scanning electron microscopy (SEM).

Key words: Bi_2O_3, Nb_2O_5, TeO_2, X ray diffraction, SEM, δ-Bi_2O_3.

Corresponding Author: LEILA LOUBBIDI

1. INTRODUCTION

Bismuth oxide has been increasingly studied for many years because of their applications in many devices, particularly in the fields of fuel cells and catalysis. It is the best known oxide ion conductor, with a conductivity of ~1 Ω-1 cm-1 at 1003 K, approximately two orders of magnitude higher than that of yttria stabilised zirconia, currently the favoured electrolyte in SOFCs [1]. His very high conductivity is attributed to the highly polarisable Bi^{3+} cations and highly disordered structure of sublattice [2-6]. However, the use of δ-Bi_2O_3 as an oxide ion conductor is limited because it is only stable in the narrow temperature range of 1002-1097 K [1].

Many experimental researches have focused of studying of the polymorphs of Bi_2O_3 phase. Bi_2O_3 presents a rich phase polymorphism, designated by α-Bi_2O_3 (monoclinic), β-Bi_2O_3 (tetragonal), γ-Bi_2O_3 (cubic, bcc), δ-Bi_2O_3 (cubic, fcc) ε-Bi_2O_3 (orthorhombic), ω-Bi_2O_3 (triclinic) [7-9].

The δ-phase can be successfully stabilized at room temperature by doping with transition metal oxides such as Re_2O_7, WO_3 and MoO_3 [10-12] or with rare-earth oxides.

The delta phase of bismuth oxide δ-Bi_2O_3 regarded as an anion deficient fluorite structure, where bismuth occupies the fcc sites, having a defect oxygen sublattice [13]. The structure of this oxygen sublattice has caused controversy.

Sillen reported on a primitive cubic phase, space group Pn-3m, obtained by quenching Bi_2O_3. This cubic structure is related to the fluorite structure but has ordered defects in the oxygen sublattice in the [111 direction. Each Bi^{3+} ion has six oxygen neighbours arranged at six corners of a cube; two oxygens at diagonally opposite corners of the cube are missing [14].

The study by Gattow and Schrőder into the *δ*-Bi_2O_3 system supposed that the cations occupied the 4*a* site and the oxygen atoms the 8*c* site with an average occupancy of 75% and a random distribution of vacancies

[15]. The high oxide ion conductivity exhibited by δ-Bi_2O_3 is consistent with a structural model in which the oxide ion sites are 75% occupied in a statistical fashion [13,15].

Willis also proposed a model where the six oxygen atoms are randomly distributed along four of the [111] directions from the regular tetrahedral sites towards the central octahedral vacant site, 32*f*, of the Fm-3m space group [16].

All three models are inconsistent with the observed experimental results, and consequently need modification to explain the complex structural changes. Studies performed by Battle *et al* [1,17,18] show the anion sublattice is a combination of the Gattow and Willis models (ie occupancy of both the 8*c* and 32*f* sites) and suggest the tendency for vacant oxygen sites to be arranged in the direction [111] configuration around the Bi atoms, as the formation of vacancy string is a well known feature of anion deficient fluorite materials.

In the present research, two new compositions (1-x)$BiO_{1.5}$-(x/4)$Nb_2Te_2O_9$ with (x=0.1, 0.2), isotype of δ-Bi_2O_3 phase, were obtained within Bi_2O_3-Nb_2O_5-TeO_2 system. The new phases are characterized by means of the X-ray diffraction and scanning electron microscopy (SEM).

2. EXPERIMENTAL PROCEDURE

2.1 Sample preparation

Samples of (1-x)$BiO_{1.5}$-(x/4)$Nb_2Te_2O_9$ (x=0.1, 0.2, 0.3, 0.6 and 0.9) were prepared by conventional solid state reaction method. High purety oxides powder α-Bi_2O_3, TeO_2 and Nb_2O_5 were used as the starting materials. The batches of suitable proportions of starting products were mixed in an agate mortar and then heated at successively higher temperatures (700, 800 and 850°C for 24h) in air with several intermediate grindings and followed by quenching. All of them are quenched to room temperature. The positions of the chemical compositions within the Bi_2O_3-Nb_2O_5-TeO_2 system are shown in Fig.1.

2.2 Instrumental methods

2.2.1 X-ray diffraction

The final products have been monitored by X-ray powder diffraction (XRD) using a Philips X'Pert PRO diffractometer and Cu-K-alpha (λ=1.5406Å) radiation. The structural refinements were undertaken from the powder data. The patterns were scanned through steps of 0.02° (2θ), between 10° and 100° (2θ) with a fixed time counting of 100s. The study of the structure is conducted by analyzing the profile of X-ray diffraction diagrams of powder with the program Fullprof [19] using the pseudo-Voight function.

2.2.2 Scanning electron microscopy

The morphology of the compositions was taken by scanning electron microscopy Zeiss Gemini supra 40 VP with a probe Oxford X-max 20mm2.

3. RESULTS AND DISCUSSIONS

3.1. Crystallographic study of synthesized compositions in the Bi2O3-Nb2O5-TeO2 system

The doping of Bi_2O_3 by 5%TeO_2 and 5%Nb_2O_5 (A: x=0.1) then by 10%Nb_2O_5 and 10%TeO_2 (B: x=0.2) allowed us to stabilize the delta phase of bismuth oxide (δ-Bi_2O_3). (Fig.1). Indexing of X-ray powder diffraction pattern for the composition B was performed by means of the computer program DICVOL [20] and TREOR [21].

- ✓ DICVOL [20]

The results show that it is a cubic system with lattice parameter a=5.4957(Å), V= 165,98($Å^3$) and a very satisfactory figure of merit M(10)=226,3.

- ✓ TREOR [21]

The diffraction peaks were indexed also in the cubic system (Fm-3m) with lattice parameter a=5,4988(Å), V=165,98($Å^3$) and M(10)=166,280.

Concerning the composition C(x=0.3), the X-ray diffraction shows that it's a mixture of Bi_3NbO_7, $Bi_2Te_2O_6$ and $BiNbO_4$. The composition D(x=0.6) is a biphasic mixtures of $Bi_2Te_2O_6$ and $BiNbO_4$.

The X-ray diffraction spectra of the composition E(x=0.9) reveals the existence of a triphases mixture: $Bi_2Nb_2O_7$, $Nb_2Te_3O_{11}$ and $BiNbO_4$.

A (x=0.1): $Bi_{0.9}Nb_{0.05}Te_{0.05}O_{1.575}$
B (x=0.2): $Bi_{0.8}Nb_{0.1}Te_{0.1}O_{1.65}$
C (x=0.3): $Bi_{0.7}Nb_{0.15}Te_{0.15}O_{1.725}$
D (x=0.6): $Bi_{0.4}Nb_{0.3}Te_{0.3}O_{1.95}$
E (x=0.9): $Bi_{0.1}Nb_{0.45}Te_{0.45}O_{2.175}$

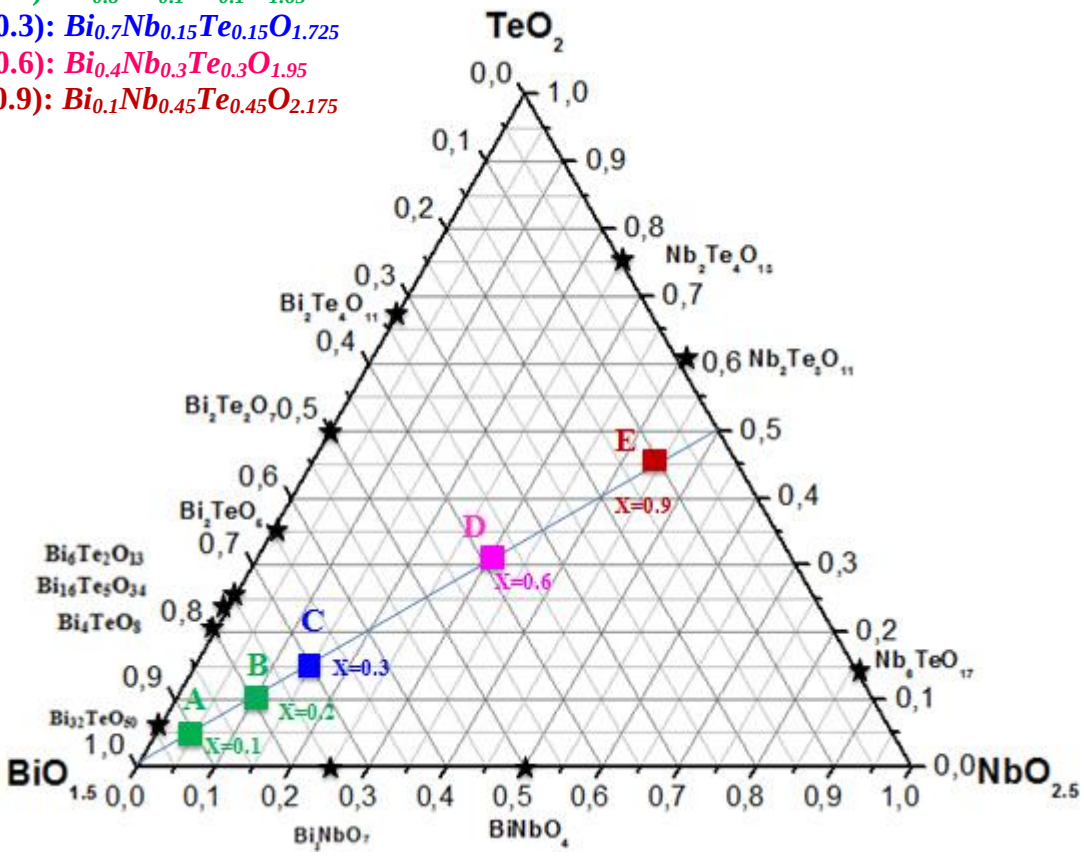

Fig 1: Localiztion of synthesized compositions in the Bi_2O_3-Nb_2O_5-TeO_2 system

Table1. Indexed powder X-ray diffraction of the B(x=0.2): $Bi_{0.8}Nb_{0.1}Te_{0.1}O_{1.65}$ composition, type δ-Bi_2O_3

hkl	Θ(°)	d_{hkl} (Å) (observed)	d_{hkl} (Å) (calculated)	%
111	14.04	3.174	3.169	100
200	16.27	2.749	2.745	41
220	23.34	1.944	1.941	33
311	27.68	1.658	1.655	26
222	29.03	1.587	1.585	7

3.2.Structural study of the $Bi_{0.8}Nb_{0.1}Te_{0.1}O_{1.65}$ composition, type δ-Bi_2O_3

The structural refinement of the composition B (x=0.2) was carried out by means of the Rietveld method using the FULLPROF program [19] integrated in WINPLOTER pack, in a field angle 10 °<2θ <99.99 ° with a step of 0.01 ° / min. All the structural parameters and the vesting conditions are summarized in Table 3.

Rietveld refinements of X-ray powder diffraction data indicate that the atomics positions are: Bi, Nb and Te in (4a). O occupied the sites 8c and 32f respectively. The reliability factors are: R_F = 2.09%, R_B = 2.99% and R_{wp}=19.1%.

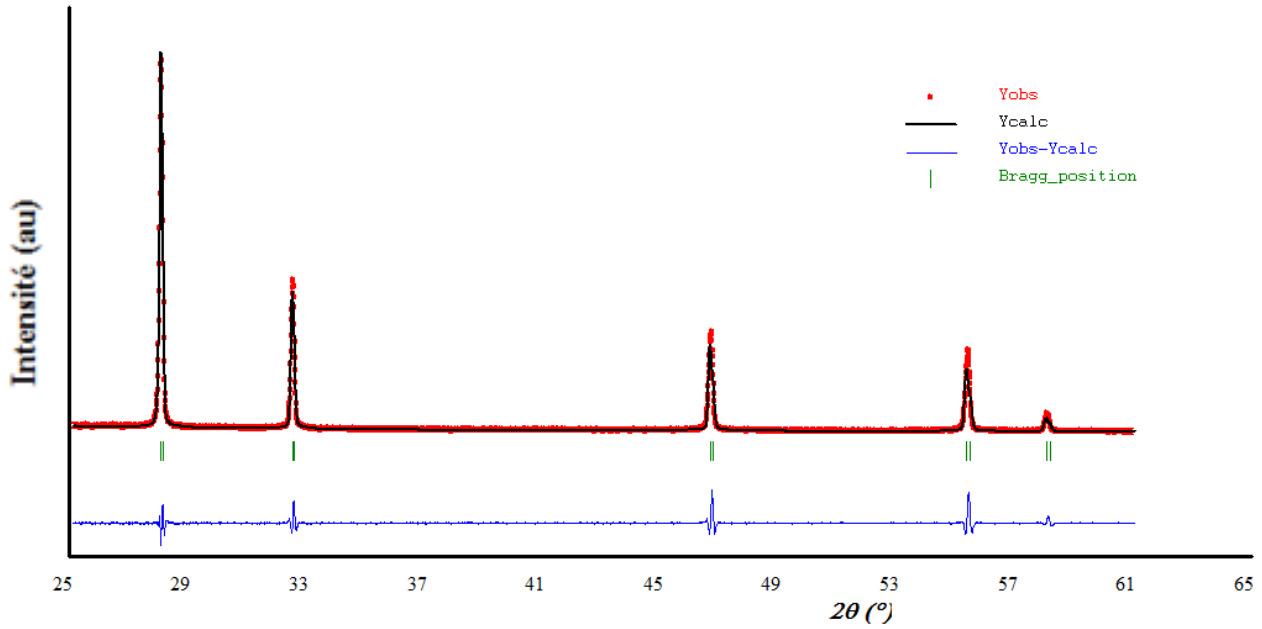

Fig 2: Final Rietveld plots of the B(x=0.2): $Bi_{0.8}Nb_{0.1}Te_{0.1}O_{1.65}$ composition, type δ-Bi_2O_3. The upper symbols illustrate the observed data (cross) and the calculated pattern (solid line). The vertical markers show calculated positions of Bragg reflexion. The lower curve is the difference diagram.

Table2. Experimental details and crystallographic data for B(x=0.2): $Bi_{0.8}Nb_{0.1}Te_{0.1}O_{1.65}$ composition, type δ-Bi_2O_3

GE	a (Å)	angular range	Step of measure	Number of refined parameters	Rp	Rwp	Rexp	R_B (%)	X^2 (%)	R_F (%)
Fm-3m	**5.499 (3)**	**10°<2θ<99.99°**	**0.01°/ min**	**64**	**19.4**	**19.1**	**10.24**	**2.99**	**1.86**	**2.09**

Table3. Atomic positions and thermal factors agitation of the $Bi_{0.8}Nb_{0.1}Te_{0.1}O_{1.65}$ composition, type δ-Bi_2O_3

Atome	Symmetry	x	y	z	Biso	Occ
Bi	4a	0.00000	0.00000	0.00000	0.1935 (3)	0.9000
Nb	4a	0.00000	0.00000	0.00000	0.1935 (3)	0.0040
Te	4a	0.00000	0.00000	0.00000	0.1935 (3)	0.0040
O1	8c	0.25000	0.25000	0.25000	0.20000	0.9000
O2	32f	0.3540(2)	0.3540 (2)	0.3540 (2)	0.20000	0.00725

Table4. Main interatomic distances (Å), angles (°) and bond valences in the B(x=0.2): $Bi_{0.8}Nb_{0.1}Te_{0.1}O_{1.65}$ composition, type δ-Bi_2O_3

Bi/Nb/Te	$O1^{(1)}$	$O2^{(1)}$	$O3^{(1)}$	$O4^{(1)}$	$O5^{(1)}$	$O6^{(1)}$	$O7^{(1)}$	$O8^{(1)}$	Valence
$O1^{(1)}$	2.38127 (8)	3.88859 (15)	3.88859 (15)	3.88859 (15)	4.76253 (15)	2.74965 (15)	2.74965 (15)	2.74965 (15)	0.46
$O2^{(1)}$	109.471 (6)	2.38127 (8)	3.88859 (15)	3.88859 (15)	2.74965 (15)	4.76253 (15)	2.74965 (15)	2.74965 (15)	0.46
$O3^{(1)}$	109.471 (6)	109.471 (6)	2.38127 (8)	3.88859 (15)	2.74965 (15)	2.74965 (15)	4.76253 (15)	2.74965 (15)	0.46
$O4^{(1)}$	109.471 (6)	109.471 (6)	109.471 (6)	2.38127 (8)	2.74965 (15)	2.74965 (15)	2.74965 (15)	4.76253 (15)	0.46
$O5^{(1)}$	180.000 (8)	70.529 (5)	70.529 (5)	70.529 (5)	2.38127 (8)	3.88859 (15)	3.88859 (15)	3.88859 (15)	0.46
$O6^{(1)}$	70.529 (5)	180.000 (8)	70.5288 (2)	70.529 (5)	109.471 (6)	2.38127 (8)	3.88859 (15)	3.88859 (15)	0.46
$O7^{(1)}$	70.529 (5)	70.529 (5)	180.000 (8)	70.529 (5)	109.471 (6)	109.471 (6)	2.38127 (8)	3.88859 (15)	0.46
$O8^{(1)}$	70.529 (5)	70.529 (5)	70.529 (5)	180.000 (8)	109.471 (6)	109.471 (6)	109.471 (6)	2.38127 (8)	0.46
$\sum Vij$									3.68

The calculation of the sum of the bond-valence (BVS) appears to indicate that the atoms (Bi, Nb, Te) occupying the same site (4a) are coordinated 8.

As shown in Fig.3, the evolution of ynit cell parameter depends to the addition of small amount of Nb_2O_5 and TeO_2 in the matrix $(BiO_{1.5})_{1-x}(NbO_{2.5})_{x/4}(TeO_2)_{x/4}$ (x=0, x=0.1, x=0.2) and shows a decrease of the lattice parameter a. This result is justified by the difference of size between the ions Bi^{3+} (1.03Å) Te^{4+} (0.97Å) and Nb^{5+} (0.74Å) [22].

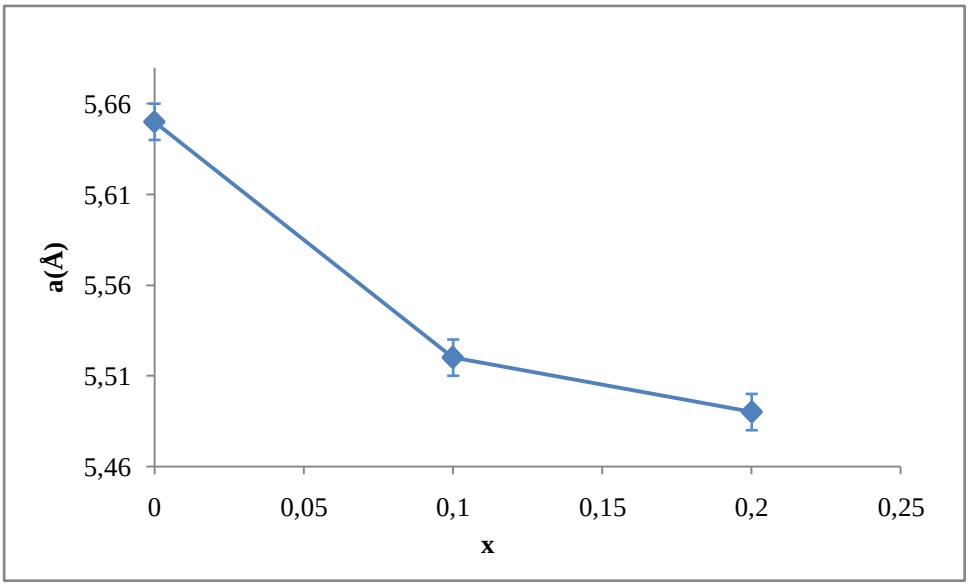

Fig 3: The variation of the lattice parameter versus x

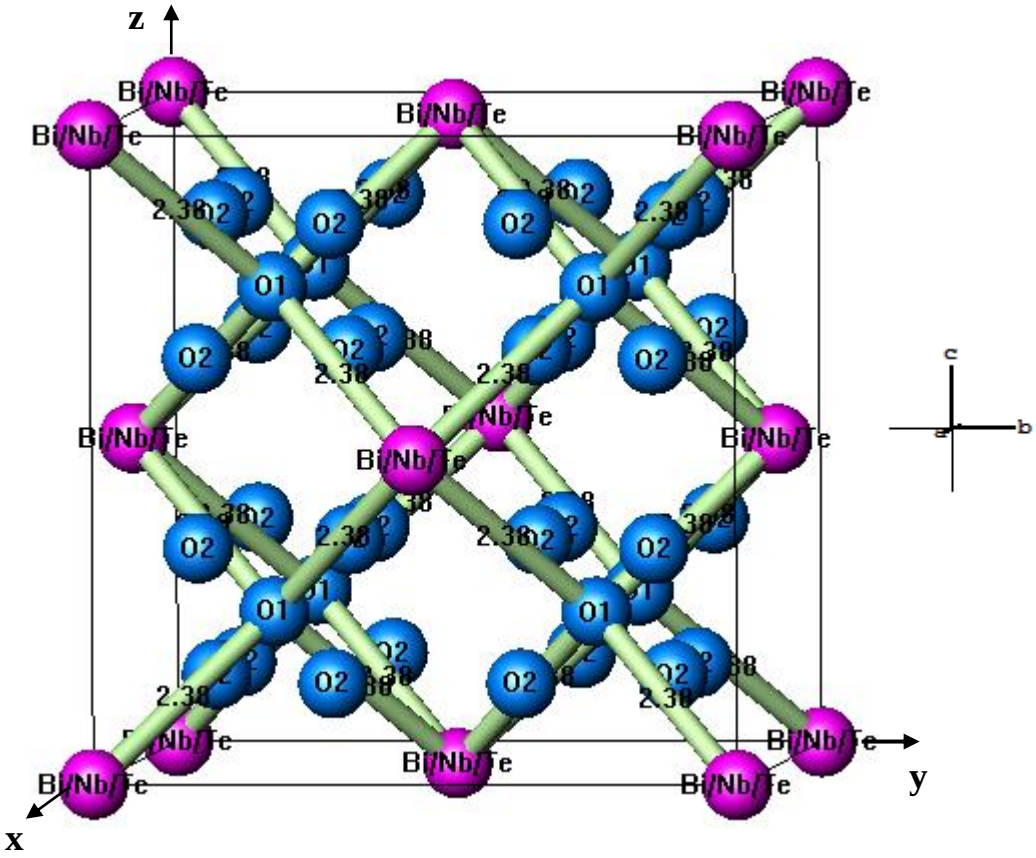

Fig 4: Structure of the B(x=0.2): $Bi_{0.8}Nb_{0.1}Te_{0.1}O_{1.65}$ composition, type δ-Bi_2O_3

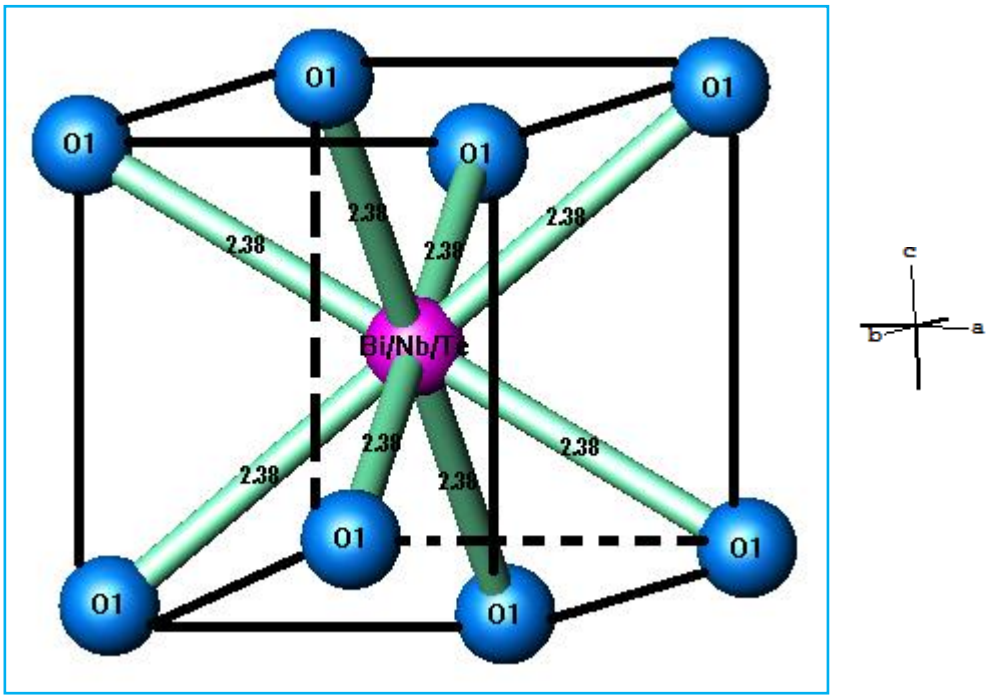

Fig 5: View of Bi/Nb/Te anionic coordination

The atoms of bismuth, niobium and tellurium are surrounded by eight oxygen atoms type 1 at a distance of 2.38 Å (Fig.5.), forming a regular cubic environment. This distance is close to the sum of the radii (1.42 +1.17) Å proposed by Shannon [22].

The oxygen atoms (O_2) are displaced from ideal (8c) wyckoff position to 32f. The maintain the stoichiometry only six oxygen anions (Bi_2O_3: Z=2) are present, there are also two vacancies per sub-unit.

We notice that the vacancies in the structure increase as the concentration of x increases from 25% (x=0), 21.25% (x=0.1) up to 17.5% (x=0.2).

3.3 Scanning electron microscopy

The SEM image of the compositions A (x=0.1): $Bi_{0.9}Nb_{0.05}Te_{0.05}O_{1.575}$ and B (x=0.2): $Bi_{0.8}Nb_{0.1}Te_{0.1}O_{1.65}$ are shown in fig 6.

Concerning the compositions A (x=0.1) and B (x=0.2), the powder is constituted of large grains with luminous contrast, in same shapes but different sizes. However, in magnifying the image, the two samples (A: x=0.1 and B: x=0.2) have the same morphology. The powder appears as a cluster of small pieces of grains. The global analysis confirms the starting composition of each sample.

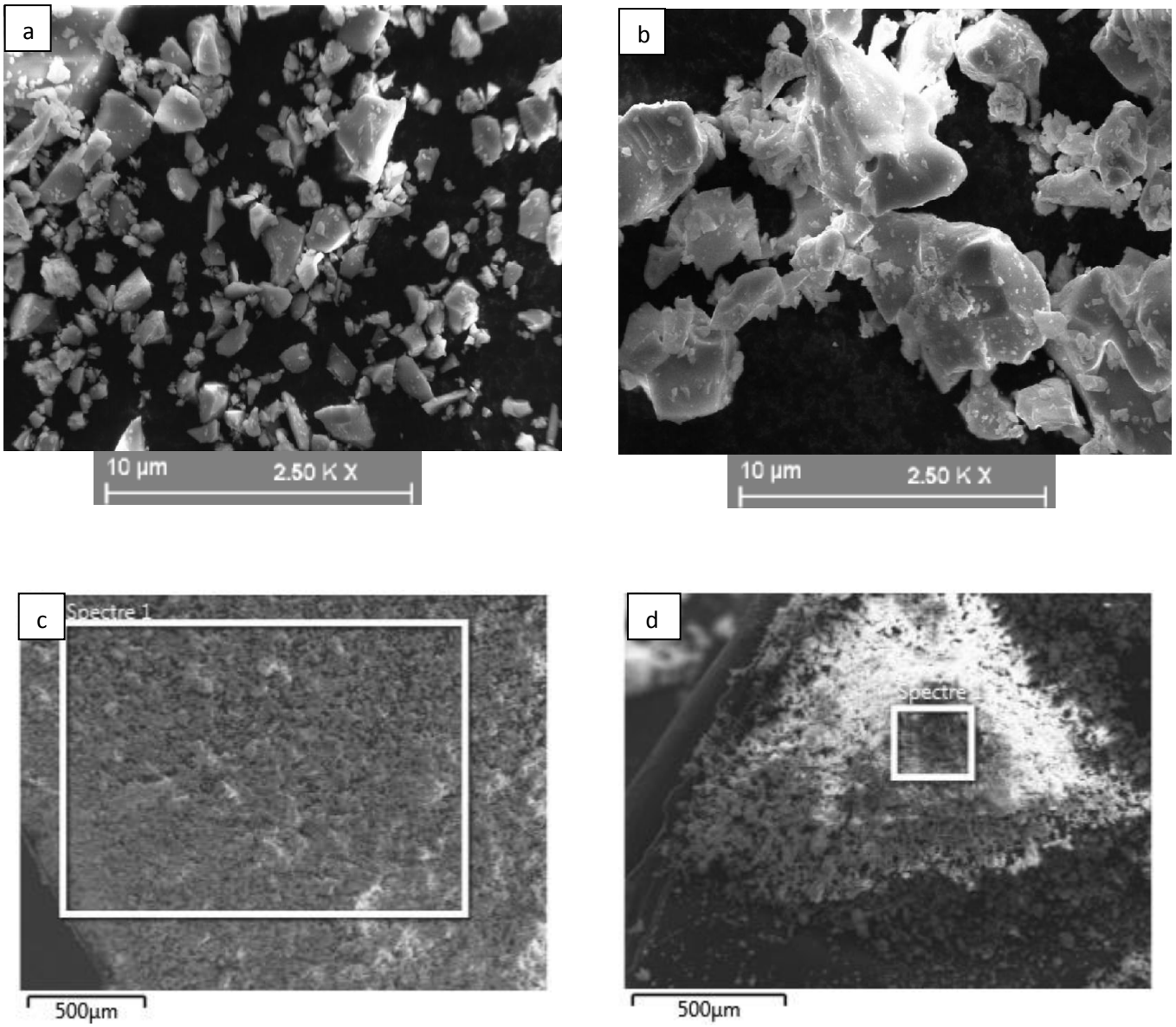

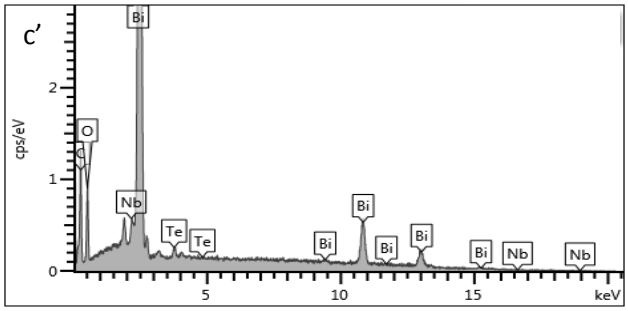

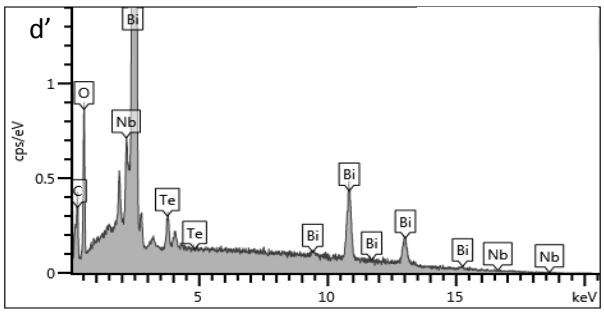

Element	Type of line	% Masse	% atomic
Nb	L series	2.41	5.16
Te	L series	3.27	5.10
Bi	Serial M	94.31	89.74
Total:		100.00	100.00

Element	Typeof line	% Masse	% atomic
Nb	L series	4.87	10.00
Te	L series	5.45	8.15
Bi	SerialM	89.68	81.86
Total:		100.00	100.00

Fig 6: *SEM micrographs illustrating the surface morphologies of the compositions a: A(x=0.1), b: B(x=0.2), c, c': global microanalysis X of A(x=0.1) and d, d': global microanalysis X of : B(x=0.2)*

4. CONCLUSION

δ-Bi_2O_3 have been stabilized by doping this oxide with Nb_2O_5 and TeO_2 with content of 5% then of 10% at room temperature.

The crystal structure was determined by means of the X-ray diffraction using the FULLPROF program [22]. The cations Bi^{3+} / Nb^{5+} / Te^{4+} occupy the same site (4a); O occupied the sites 8c and 32f respectively in the fluorite structure.

The global analysis obtained by the Scanning electron microscopy confirms the starting composition of each sample.

5. REFERENCE

[1] Thompson Maria, Thesis, University of Birmingham, (2010).
[2] Watanabe, Solid State Ionics, 40-41, 889-892, (1990).
[3] N. Jiang, R.M. Buchanan, F.E.G. Henn. A.F. Marshall, D.A. Stevenson, E.E. Wachsman, Mater. Res. Bull., 29, 247-254, (1994).
[4] E.D. Wachsman, S. Boyapati, M.J. Kaufman, N. Jiang, J. Am. Ceram. Soc., 83, 1964-1968, (2000).
[5] E.D. Wachsman, G.R. Ball, N. Jiang and D.A. Stevenson, Solid State Ionics, 52, 213-218, (1992).
[6] S. Boyabati, E.D. Wachsman and B.C. Chakoumakos, Solid State Ionics, 138, 293-304, (2001).
[7] N. M. Sammes, G. A. Tompestt, H. Nafe, F. Aldinger, J. Eur. Ceram. Soc. 19 (1999) 1801.
[8] T. Takahashi, H. Iwahara, Y. Nagai, J. Appl. Electrochem. 2, 97 (1972).
[9] S. Nakayama, Ceram. Int. 28, 907 (2002).
[10] Neeraj Sharma, Ray L. Withers, Kevin S. Knight, Chris D. Ling, Journal of Solid State Chemistry, Volume 182, Issue 9, Pages 2468–2474, (2009).
[11] Akiteru Watanabe, Masami Sekita, Solid State Ionics, Volume 176, Issues 31–34, Pages 2429–2433, (2005).
[12] Neeraj Sharma, Rene B. Macquart, Mogens Christensen, Maxim Avdeev, Yu-Sheng Chen, Chris D.Ling, Journal of Solid State Chemistry, 182(2009)1312‑1318
[13] Harwig, H. A. Z. Anorg. Chem. 444, 151, (1978).
[14] Sillen, L. G. Ark. Kemi Mineral. Geol. 12A (1937) 1.
[15] Gattow, G.; Schutze, D. Z. Anorg. Allg. Chem. 328, 44, (1964).
[16] Willis, B. T. M. Acta. Cryst. 18, 75, (1965).

[17] P. D. Battle, C. R. A. Catlow, J. W. Heap, and L. M. Moroney, *J. Solid State Chem*., **63** 8 (1986).
[18] P. D. Battle, C. R. A. Catlow, J. W. Heap, and L. M. Moroney, *J. Solid State Chem*., **67** 42 (1987).
[19] Program Full Prof.2k (Version 5.30 - Mar2012-ILL JRC).
[20] Program Dicvol 04, Boultif, A. & Louer, D. J. APPL. CRYST. 37, 724-731, (2004).
[21] Program Treor 90, Université de Stockholm (Sweden), (1990).
[22] R.D. Shannon, Acta Crystallogr, A32, 751, (1976).